A Brownian Dynamics Simulation of an Acyl Chain and a *trans*-Parinaric Acid Molecule Confined in a Phospholipid Bilayer in the Gel and Liquid-Crystal Phases

M. X. Fernandes,[†] J. García de la Torre,[‡] and M. A. R. B. Castanho*[,†,§]

Departamento de Química e Bioquímica da Faculdade de Ciências da Universidade de Lisboa, Campo Grande, Ed. C8-6° Piso, 1749-016 Lisboa, Portugal, Departamento de Química-Física, Facultad de Química, Universidad de Murcia, 30071 Murcia, España, and Centro de Química-Física Molecular, Instituto Superior Técnico, Av. Rovisco Pais, 1049-001 Lisboa, Portugal

Received: July 6, 2000; In Final Form: September 19, 2000

A Brownian dynamics simulation of a saturated 16 C atom acyl chain, in a environment that reproduces a phospholipid bilayer in the gel phase, is presented. The simulation was performed using simple mean-field potentials, and the results were compared with experimentally obtained results for similar phospholipid acyl chains. With the appropriate choice of parameters, equilibrium and dynamical properties are recovered from our simulations and they present excellent agreement with experimentally determined values. We also performed a simulation of *trans*-parinaric acid, a fatty acid molecule widely used to probe the existence of lateral domains in phospholipid bilayers. The results of this simulation confirm the peculiar behavior of *trans*-parinaric acid when it is placed in different environments and reinforce the validity of the Brownian dynamics technique to simulate membrane model systems.

Introduction

Dispersions of phospholipid bilayers in water can exhibit different phases. These depend on temperature and on the nature of phospholipids, namely acyl chain length and degree of unsaturation. Among the phases of phospholipid bilayers[1] one could refer the liquid-crystal phase, L_α, which is characterized by its fluid nature with high level of flexibility and low level of order assigned to the acyl chains of phospholipids.[1] Another important phase of bilayers is the gel phase, L_β, which presents regular packing and significant order for the acyl chains of phospholipids.[1]

Several biological processes depend on the physical characteristics of membrane bilayers. The most relevant biologically is the L_α phase, but intercalated gel phases have been detected experimentally,[2] and recent studies prove that lateral domain existence in cell membranes is important to gene expression,[3] binding and activation of enzymes,[4] and cell division.[5] Experimental structural and dynamical information for the liquid-crystal phase is scarce, mainly due to problems posed by the "disordered" nature of bilayers. Nevertheless, there is a lot of information concerning that physical phase produced by simulation techniques (e.g., for a review, see ref 6). Conversely, there is a lot of experimental structural information about the gel phase,[7−10] but it has received little attention by theoreticists and there are few simulation works about the L_β phase, possibly due to its minor biological relevance.

There are some molecular dynamics (MD) simulation works reported concerning the gel phase. Some of these are incidental,[11,12] because the purpose was to simulate a bilayer in the liquid-crystal phase, but due to an inconvenient parametrization of force fields a bilayer with gel-phase-like properties was attained, even above the phase transition temperature of simulated phospholipids. Some deliberate attempts to simulate a gel phase are also reported.[13−15] All these MD simulations recover, with good agreement, experimentally determined properties such as area per lipid, acyl chain tilt angle, or transversal atom distribution. However, there are some results that clash with experimental observations, namely a pleated arrangement of acyl chains in the center of the bilayer[13,14] when a parallel arrangement is expected on the basis of X-ray diffraction studies.

We propose a mean-field approach using Brownian dynamics (BD) simulation with atomic level detail to model a 1,2-dipalmitoyl-3-*sn*-glycerol-phospatidylcholine (DPPC) bilayer system in the L_β phase. In this approach the influence of neighboring molecules is represented by three simple potentials.[16,17] A BD simulation, opposed to the all atom description used in MD, allows the performance of long time range simulations, in which many relevant biological processes take place, instead of only a few hundred picoseconds MD simulations. Obviously, because a single molecule is described in our BD runs, global motions of membrane systems or cooperative effects of molecules cannot be simulated. However, structural and dynamical information of simulated molecules can be obtained and its validity assessed.

After appropriate parametrization of the mean-field potentials, to recover experimentally determined properties of acyl chains in a DPPC gel-phase bilayer, we simulated, in the same environment, a *trans*-parinaric acid molecule, *t*-PnA, which was also simulated in the environment of a DPPC liquid-crystal phase. *t*-PnA is a widely used molecule to probe membranes lateral organization or domain formation.[18,19] The detection of lateral domains by *t*-PnA is based on the high sensitivity of the probe fluorescence parameters to lipid density.[20] BD simulation

* Author to whom correspondence should be addressed at Centro de Química-Física Molecular, Instituto Superior Técnico, Av. Rovisco Pais, 1049-001 Lisboa, Portugal. Telephone: +351218419248. Fax: +351218464455. E-mail: pcmcastanho@popsrv.ist.utl.pt.

[†] Departamento de Química e Bioquímica da Faculdade de Ciências da Universidade de Lisboa.

[‡] Departamento de Química-Física, Facultad de Química, Universidad de Murcia.

[§] Centro de Química-Física Molecular, Instituto Superior Técnico.

10.1021/jp002415c CCC: $19.00
Published on Web 11/11/2000

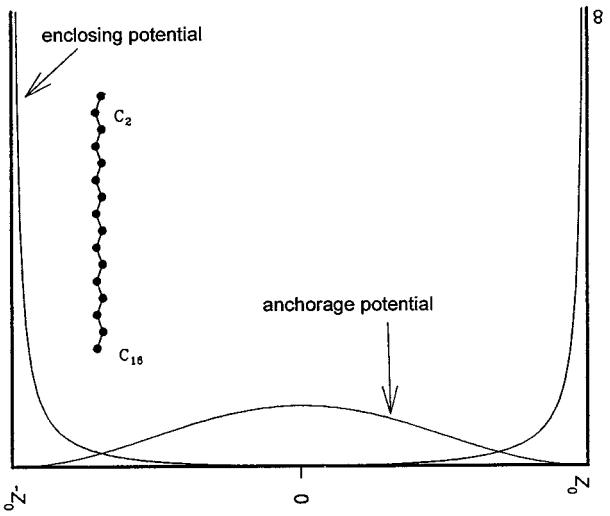

Figure 1. The simulated acyl chain and the profile of mean-field potentials in the phospholipid bilayer.

results were compared with experimental data for *t*-PnA in liquid-crystal and gel phases. Some conclusions are taken that could bring about light on the complex decay kinetics of fluorescence anisotropy of *t*-PnA.

Results presented here validate the BD approach to simulate a bilayer system in the L_β phase. Furthermore, due to the simplicity of the mean-field potentials used, and suitable description of simulated molecules, long time range simulations could be performed and structural and dynamical results withdrawn for membrane components or probes located in a membrane environment.

Model and Simulation Procedures

Model. The system that we simulate has 16 spherical elements joined by a frictionless connector and models the structure of a 16 C atom acyl chain. This molecule is placed in a model membrane of finite thickness and none of spheres, which represent methyl and methylene groups, can trespass the simulated membrane boundaries which means that the movement is confined in the *z* direction (see Figure 1). One of the spheres represents the C atom that would bond to the glycerol moiety. In that case the simulated chain would represent one of the acyl chains of a phospholipid. This is our purpose, although the simulated chain does not represent specifically the *sn*-1 or *sn*-2 chain, but the average characteristics, namely transverse location profiles of C atoms or segmental order parameters, of both. It is known that *sn*-1 and *sn*-2 chains are not exactly equivalent in a gel-phase bilayer of DPPC.[9] The chain-model generally extends itself in one of the layers of the bilayer, meaning between $[0, z_0]$ or $[-z_0, 0]$.

In the case of *t*-PnA we used an 18 element chain that reproduces the structure of that fatty acid, which has 4 conjugated double bonds at positions 9, 11, 13, and 15 (see Figure 2). The carboxyl group was substituted by a pseudo-atom that tends to be anchored at the membrane boundary. Once again the movement of this molecule is confined in the *z* direction.

Intramolecular Energetics. The internal energy of simulated molecules has contributions resulting from stretching, bending, torsional, and nonbonded interaction energy. More clearly, the stretching potential maintains the bond length between any two consecutive elements of a simulated molecule and it has a harmonic type expression in l (l is the distance between two consecutive elements). The angle between any three consecutive

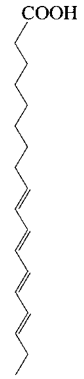

Figure 2. Structure of *trans*-parinaric acid.

elements of simulated molecules is maintained by the bending potential that also has a harmonic-type expression in α (α is the angle formed by three consecutive elements). The torsional potential which is represented by a power series of cos ϕ (ϕ is the dihedral angle formed by four consecutive elements) was introduced by Ryckaert and Bellemans,[21] and it accounts the contribution of dihedral angles for the total internal energy of the simulated molecule. The nonbonded potential represents the contributions due to van der Waals interactions between elements i and j ($j \geq i + 4$). The expression for this potential is

$$V_{\mathrm{LJ}} = 4\epsilon\left(\left(\frac{\sigma}{r_{ij}}\right)^{12} - \left(\frac{\sigma}{r_{ij}}\right)^{6}\right)$$

In the case of *t*-PnA we have to perform slight modifications in the expression for the torsional potential due to the presence of double bonds. The torsional potential expression for dihedral angles around sp^2-sp^3 C atoms is given by[22]

$$V_\phi = c_1(1 + \cos\phi) + c_2(1 + \cos(2\phi)) + c_3(1 + \cos(3\phi))$$

and the rotation around sp^2-sp^2 C atoms is prevented using the expression given by[22]

$$V_\phi = k_\phi(\cos\phi - \cos\phi_0)^2$$

where c_i and k_ϕ are constants, ϕ is the dihedral angle, and ϕ_0 is 0° (all double bonds are in trans conformation). The magnitudes used for all the above-described potentials are given elsewhere.[16,22]

Mean-Field Potentials. The mean-field that simulates a bilayer environment has contributions resulting from (1) enclosing potential that emulates the finite thickness of the bilayer and also the hydrophilic nature of membrane interfaces; (2) the anchorage potential that places elements which interact favorably with membrane interfaces in their vicinity; and (3) the orientational potential which emulates the anisotropic medium of a bilayer and the ordering effect induced by acyl chains in neighboring molecules. The enclosing potential acts on all spheres but the one that represents the C atom that would bond to the glycerol moiety, in the case of phospholipid acyl chains, or the C atom of the carboxylic group in the case of *t*-PnA. Conversely, the anchorage potential acts only on the sphere that represents the C atom that would bond to the glycerol moiety, in the case of phospholipid acyl chains, or the C atom of the carboxylic group in the case of *t*-PnA. The expressions of these potentials were presented elsewhere.[16]

In the L_β phase, acyl chains of phospholipids present a tilt angle relative to the normal of the bilayer.[9] To reproduce this

feature the simulated chains are preferentially orientated along an axis that is tilted relative to the bilayer normal. The orientational potential expression is

$$V_{\text{orient}} = -\frac{3}{2}kTK_{\theta}(z)(\cos^2(\theta_i - \theta_{\text{tilt}}) - 1)$$

where θ_{tilt} is the tilt angle, θ_i is the angle formed by the segment that joins the atoms $C_{i-1}-C_{i+1}$ and the bilayer normal, k is the Boltzmann constant, T is the absolute temperature, and $K_{\theta}(z)$ is the field strength of the orientational potential. $K_{\theta}(z)$ is constant throughout the simulated bilayer. This is the main difference between the mean-field potentials that describe the L_{α} and the L_{β} phases. In the L_{α} phase, $K_{\theta}(z)$ is not constant throughout the membrane—instead it changes linearly with z,[16] reflecting the different packing of acyl chains in bilayers revealed by neutron diffraction studies,[23] and θ_{tilt} is zero. Concerning all mean-field potentials there are differences in their magnitudes. The comparison between magnitudes of potentials used in the simulation of a L_{β} phase relative to those used in the simulation of a L_{α} phase[16] shows that $K_{\theta}(z)$ is higher, K_{anch} is higher, and K_z is lower.

Parametrization of Mean-Field. The mean-field potential magnitudes were the object of a systematic search. Results obtained for each particular set of values were compared with experimental data and the set that gave the best fit was chosen to be used throughout the remaining of the work. For instance, our search shows the following: a higher value of the orientational potential will lead to a general raise in the segmental order parameters, $-S_{\text{mol}}(i)$; a higher value of the anchorage potential will produce a small raise of $-S_{\text{mol}}(i)$ in the region near the interface; and a higher value of the enclosing potential has an effect of diminishing the $-S_{\text{mol}}(i)$ near the bilayer midplane. A more detailed description of the choice problem for the parameters magnitudes was presented elsewhere.[16]

The anchorage potential field constant was set to 1.5×10^{-1} kJ mol^{-1}; the enclosing potential field constant has a value of 12.92 kJ Å^2 mol^{-1}; the orientational potential field constant employed was 7.8×10^{-1} kJ mol^{-1}; and the tilt angle was 17°.[9] With this choice of parameters we recovered the experimentally determined average positions of C atoms,[9] expected segmental order parameters,[24] and experimentally determined percentage of gauche defects[25] (see below).

The simulations were performed for a bilayer half-thickness of 23 Å,[9] at 293 K, a temperature for which DPPC is in the L_{β} phase.[9]

The simulations of *t*-PnA were performed in the same conditions presented above for the L_{β} phase. For the simulation of *t*-PnA in the L_{α} phase, the anchorage potential constant, K_{anch}, used was 9.7×10^{-2} kJ mol^{-1}, the enclosing potential constant, K_z, takes the value of 19.38 kJ Å^2 mol^{-1}, and the orientational potential constant, $K_{\theta}(z)$, was set to 6.2×10^{-2} kJ mol, at $|z| = z_0$, and 5.2×10^{-2} kJ mol^{-1} at the $z = 0$.[16] The simulations were done with a membrane half-thickness, z_0, of 20 Å,[9] at 324 K, well above the transition phase temperature (314 K) of DPPC.

Dynamics Algorithm. The trajectories of a single molecule, in each case, were simulated, with a computation time step of 10 or 4 fs (for *t*-PnA) and a total trajectory time of 200 ns, using a method based on the BD algorithm of Ermak-McCammon[26] with the predictor-corrector modification introduced by Iniesta and García de la Torre.[27]

When simulating dynamic properties, we took into account the hydrodynamic interaction (HI) between elements of our system. For this purpose we used the modified Oseen tensor[28,29] which corrects the effects of a nonpoint-like nature of friction elements and eventual overlapping. When simulating equilibrium properties, HI was neglected because equilibrium magnitudes do not depend on the rate of dynamic processes. BD without HI is considerably less computation time-consuming than BD with HI.

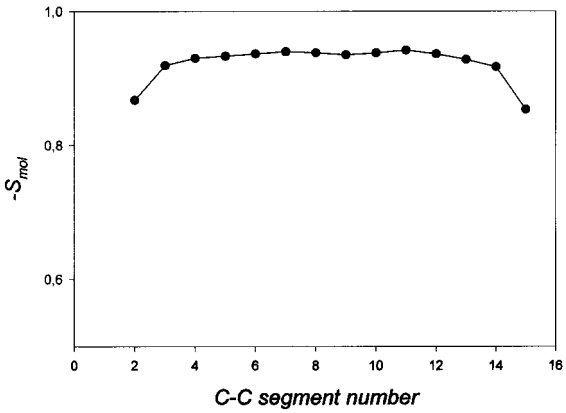

Figure 3. C−C segmental order parameter of simulated acyl chain.

Results and Discussion

DPPC. One can see in Figure 3 the segmental order parameters, $-S_{\text{mol}}(i)$, plotted against the carbon position of the acyl chain (position 2 is closer to the interface and position 15 is closer to the bilayer center). This parameter is an indication of the relative order of acyl chains, and it is associated with the orientation of the segment that joins atoms $C_{i-1}-C_{i+1}$ and the plane of the bilayer. Its expression is

$$-S_{\text{mol}}{}^{(i)} = \left\langle \frac{3\cos^2\beta_i - 1}{2} \right\rangle$$

where β_i is the angle formed by the bilayer normal and the vector that joins atoms $C_{i-1}-C_{i+1}$, and the brackets denote an average over the entire trajectory. The $-S_{\text{mol}}(i)$ can assume values between −0.5 (orientation parallel to the bilayer plane) and 1 (orientation perpendicular to the bilayer plane). Figure 3 shows that this parameter has value around 0.93 for all inner positions but extremity positions present lower values. This indicates a extremely high order for inner positions and a little less for extremity positions. The value around 0.93 is the one expected for an acyl chain tilt angle of 17°. The apparent odd symmetry between the values of $-S_{\text{mol}}(i)$ for atoms C_2 and C_{15} can be explained by the fact that these values depend strongly on rotational freedom of molecular segments. The degree of rotational freedom is higher for atoms situated near the ends of a chain. In a real phospholipid the C_1 atom will not occupy a terminal position (as it happens in the simulated chain), but instead it would be bonded to a glycerol moiety, and that is why C_2 and C_{15} present similar values for $-S_{\text{mol}}(i)$ in the case of the simulated chain. The same reason also explains the similarity of values for the dihedral angle population in trans conformation presented below.

Figure 4 shows the percentages of trans conformation for each dihedral angles of simulated acyl chain. The dihedral angles were considered to be in that conformation when they assumed values of 0° ± 60°, meaning until they crossed the dihedral potential barrier. It can be seen, from Figure 4, that percentages of trans conformation are close to 100% except for extremity dihedral angles, which is expected since the atoms involved in the formation of extremity dihedral angles present more rotational freedom. These values are in good agreement with

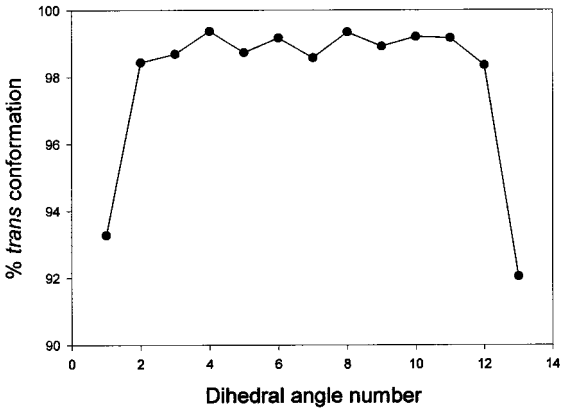

Figure 4. Simulated acyl chain dihedral angle population in trans conformation.

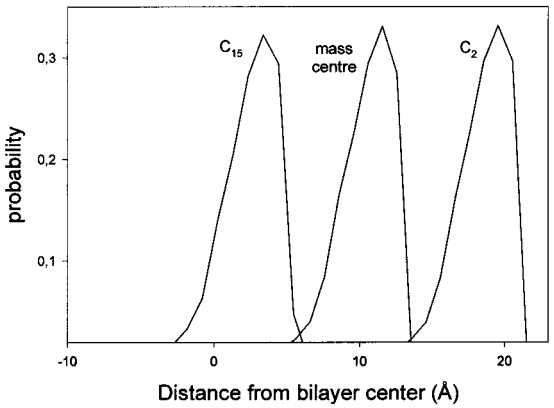

Figure 5. Density profile for the transverse position of selected C atoms and mass center from simulated acyl chain.

TABLE 1: Average Transverse Positions of Acyl Chain Carbon Atoms in L_β Phase

	distance from bilayer center (Å)	
atom	simulation	experimental[a]
C_2	19.00 ± 1.0	18.8 ± 1.0
C_3	17.78 ± 1.0	
C_4	16.54 ± 1.0	16.2 ± 0.6
C_5	15.32 ± 1.0	15.9 ± 0.6
C_6	14.08 ± 1.0	
C_7	12.85 ± 1.0	
C_8	11.62 ± 1.0	
C_9	10.39 ± 1.0	10.1 ± 1.0
C_{10}	9.15 ± 1.0	
C_{11}	7.93 ± 1.0	
C_{12}	6.69 ± 1.0	
C_{13}	5.48 ± 1.0	
C_{14}	4.24 ± 1.0	4.1 ± 0.6
C_{15}	3.08 ± 1.0	3.0 ± 0.6

[a] Experimental results taken from ref 9.

experimentally determined percentages[25] and also with simulation results obtained with other techniques.[14,15] Percentages of trans conformation for inner dihedrals present a curious odd−even effect (not justifiable by statistical fluctuations) that was also reported in other related situations.[16,30] In Figure 5 the density profile is represented for the transverse position of two C atoms and for the mass center of the acyl chain. The density profile is similar in every case concerning the width of the distribution. This is a clear indication that dispersion around the average position of a C atom is due to movements of the whole chain and not to fluctuations of that particular C atom. The average positions of C atoms are presented in Table 1, and

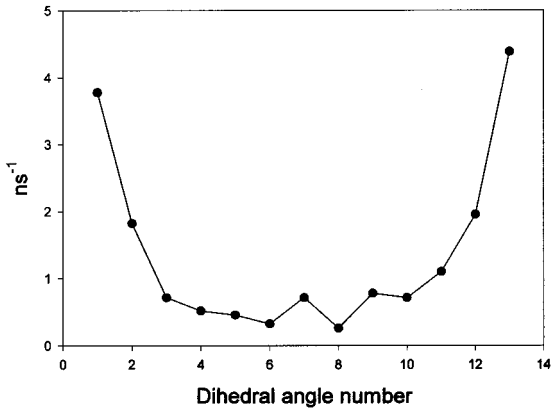

Figure 6. Dihedral angle transition rate for the simulated acyl chain.

they are in excellent agreement with experimentally determined values.[9]

Figure 6 shows the results of dihedral angle conformation transition rates, trans−gauche for the simulated chains. We considered that a transition occurred when the dihedral angle value overcame the potential barrier and crossed the corresponding dihedral angle potential local minimum. This way temporary leaps are not counted as true transitions. Assuming that the transitions are independent, the transition rate is obtained by division of the number of transitions by the total time spent in that conformation. Inspection of Figure 6 shows that inner dihedral angles present lower values for transition rates than extremity dihedral angles, which is explained by higher rotational freedom of extremity atoms. These values are in agreement with experimental values reported.[25] The gauche−trans rates are 2 orders of magnitude higher than trans−gauche (results not shown), and this can be assigned to a lower potential barrier when dihedral angles change their conformation from gauche to trans.

***trans*-Parinaric Acid.** The results presented here for t-PnA are referred to the chromophore end-to-end vector. This vector is the one that joins atoms C_9 and C_{16}, the first and the last involved in double bond formation. The four conjugated double bonds are responsible for the fluorescence characteristics of t-PnA.

Simulation results show that *t*-PnA presents very distinct behavior in L_α and L_β phases. We obtained for the $\langle P_2(\cos\theta)\rangle$ parameter (P_2 is the second Legendre polynomial, θ is the angle formed by the end-to-end chromophore vector and the bilayer normal, and $\langle ... \rangle$ denotes an average over the entire simulated trajectory) a value of 0.38 in the L_α and of 0.91 in the L_β phase. These values agree quite well with experimentally determined values, for the same parameter in identical conditions,[16] which are 0.42 and 0.91 for the L_α and L_β phases, respectively.

Figure 7 presents the simulation results for the probability distribution function of θ (which keeps the above meaning) in the L_α and L_β phases and the experimental results for the L_β phase. Experimental data[31] was obtained by a conjugation of UV−vis absorption spectroscopy to calculate $\langle P_2\rangle$ (from dichroic ratio measurements in oriented DPPC multilayers deposited over a quartz substrate) and fluorescence spectroscopy to calculate $\langle P_4\rangle$, as proposed by Kooyman et al.[32] under the framework of the Strong Collision Model, assuming equal anisotropies in vesicles and planar bilayers. The experimental data was corrected for both the effects of light refraction in the sample and light polarization with respect to the plane of incidence (corrections using Snell's and Fresnel's laws, respectively). The density probability functions calculation from the experimental obtained values of $\langle P_2\rangle$ and $\langle P_4\rangle$ was carried out by maximizing

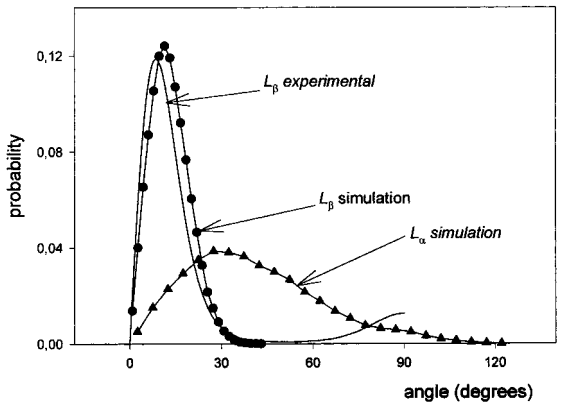

Figure 7. Density profile for the angle that the chromophore of *t*-PnA makes with phospholipid bilayer transverse plane.

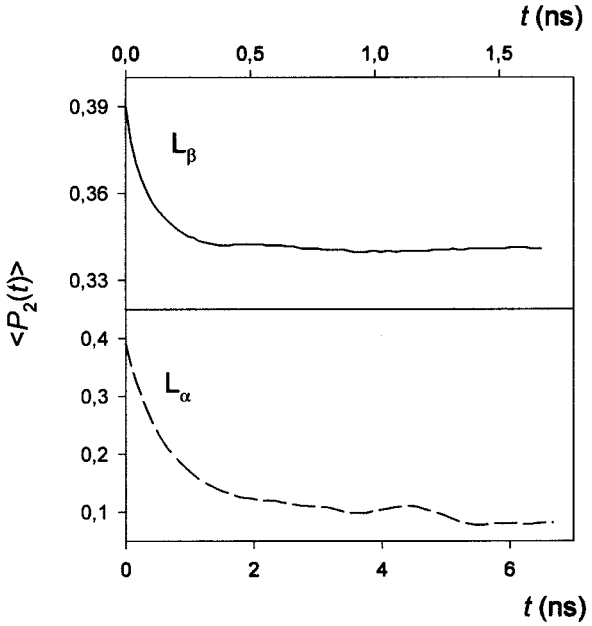

Figure 8. Rotation correlation analysis for the chromophore of *t*-PnA.

the information entropy of the distribution.[33] The suitability of this methodology is validated by its application to the simulated data in this paper. In that situation the method recovered correctly the density probability function of the chromophore angle obtained from simulated trajectories (results not shown), starting with input values of $\langle P_2 \rangle$ and $\langle P_4 \rangle$ for the same simulation.

It can be seen that there is a very good agreement between simulation and experiments. Comparison of results obtained for the L_α and L_β phases indicate clearly that the chromophore has more flexibility in the L_α phase, since it spans a wider domain of orientations, which is expected since in the liquid-crystal phase the acyl chains are more disordered than in the gel phase.[9] Because it is not possible to obtain experimentally the results for the distribution function of θ in the L_α phase, the simulation results stand as an indicator of the behavior of *t*-PnA.

Figure 8 presents the results for the $\langle P_2(t) \rangle$ decay, of the chromophore end-to-end vector, that outcome from *t*-PnA simulations. This decay can be compared with experimental fluorescence anisotropy decay, $r(t)$, of *t*-PnA. This is possible only because absorption and emission transition moments are almost collinear.[34] We normalized the $\langle P_2(t) \rangle$ decay making $\langle P_2(0) \rangle = r(0)$, with $r(0) = 0.39$.[35] The $\langle P_2(t) \rangle$ decays were fitted to a multiexponential with DISCRETE[36,37] and the results are

TABLE 2: Parameters From the Fit of Multi-exponential Functions to $\langle P_2(t) \rangle$ Simulated Decays. Fitted Equation Was $\langle P_2(t) \rangle = a_0 + a_1 \exp(-b_1 t) + a_2 \exp(-b_2 t) + ...$

DPPC phase	parameter	simulation	experimental
L_β	a_0	0.339	0.34[b]
	a_1	0.018	
	b_1	0.219 ps	
	a_2	0.032	
	b_2	0.053 ps	
	τ_{mean}[a]	98.5 ps	<100 ps
L_α	a_0	0.094	0.07[b]
	a_1	0.285	
	b_1	797 ps	
	τ_{mean}	797 ps	1100 ps

[a] τ_{mean} was calculated using the formula $(a_1/b_1 + a_2/b_2)/(0.39 - a_0)$. [b] Experimental values of r_∞. All experimental values from ref 19.

in Table 2. It can be seen that the mean correlation time in the gel phase is smaller than the one corresponding to the fluid phase. Similar results were found experimentally,[19] but the justification that fast trans−gauche isomerizations, in the saturated part of *t*-PnA, could account for this result is not plausible. In fact, trans-gauche isomerizations in the gel phase are slower than in the liquid-crystal phase (see above and ref 16). We think that because acyl chain packing is tighter in the gel phase any slight deviation is more rapidly "corrected" by the bilayer. This would explain the smaller correlation time in the gel phase, and also the bigger residual anisotropy value since large deviations from average orientation are not possible. Table 2 also shows that the $\langle P_2(t) \rangle$ decay in the gel phase is more complex than in the liiquid-crystal phase, having two components in the first case and just one in the latter. The values of a_0 obtained from fit to simulated decays agree very well with experimental results of residual anisotropy, r_∞, but average correlation times, for the same decays, are less concordant though following the same trend. In the experimental work used for comparison,[19] it was not possible to obtain correlation times lower than 100 ps or to separate components of any decay. The presented results for correlation times are an example of how simulations can help explaining results that were left unanswered due to the inaccessibility of some experimental techniques to finer time or space domains.

Conclusions

We proposed previously a mean-field description of a liquid-crystal phase DPPC bilayer,[16] that was extended here to a gel-phase DPPC bilayer. The mean-field description was used in Brownian dynamics simulations, and results fully confirm the validity of our proposal. The simplicity of the description used allows long time range simulations. Conformational properties of acyl chains such as order parameters, C atom distribution profiles or percentage of dihedral angle populations can be recovered and are in very good agreement with experimental results. Dynamic properties, such as dihedral angle transition rates or diffusion coefficients can also be recovered.

The simulation of *t*-PnA, a fluorescent fatty acid widely used to probe lateral lipid domains in bilayers and membranes, reinforces the validity of the mean-field description as results agree very well with the ones obtained experimentally. Furthermore, simulation results help to explain shadowed areas of fluorescence anisotropy decay kinetics.

The proposed approach is useful to simulate, by Brownian dynamics, conformational and dynamical properties of acyl chains or related molecules in the gel phase of DPPC. The simulation can be done not only to corroborate experimental

findings, or maybe to enlighten some of them, but also most probably with predictive purpose, such as with the worked example of *t*-PnA.

Acknowledgment. We thank Fundação para a Ciência e Tecnologia (Portugal) for Grant PRAXIS XXI BD/9393/96 to M.X.F. and funding (project PRAXIS XXI/P/SAU/14025/1998); Dirección General de Investigación Científica y Técnica (MEC, Spain) for Grant PB96-1106 and Fundación Séneca (Región de Murcia, Spain) for Grant 01258/CV/98 to J.G.T.

References and Notes

(1) Lewis, R. N. A. H.; McElhaney R. N. In *The Structure of Biological Membranes*; Yeagle, P., Ed.; CRC Press Inc.: Boca Raton, FL, 1992; p 73.

(2) Braganza, L. F.; Worcester, D. L. *Biochemistry* **1986**, *25*, 2591.

(3) Norris, V.; Madsen, M. S. *J. Mol. Biol*. **1995**, *253*, 739.

(4) Yang, L.; Glaser, M. *Biochemistry* **1996**, *35*, 13966.

(5) Welby, M.; Poquet, Y.; Tocanne, J. F. *FEBS Lett.* **1996**, *384*, 107.

(6) Tieleman, D. P.; Marrink, S. J.; Berendsen, H. J. C. *Biochim. Biophys. Acta* **1997**, *1331*, 235.

(7) Sun, W. J.; Suter, R. M.; Knewtson, M. A.; Worthington, R. C.; Tristram-Nagle, S.; Zhang, R.; Nagle, J. F. *Phys. Rev. E* **1994**, *49*, 4665.

(8) Büldt, G.; Gally, H. U.; Seelig, J.; Zaccai, G. *J. Mol. Biol.* **1979**, *134*, 673.

(9) Zaccai, G.; Büldt, G.; Seelig, A.; Seelig, J. *J. Mol. Biol.* **1979**, *134*, 693.

(10) Wiener, M. C.; Suter, R. M.; Nagle, J. F. *Biophys. J*. **1989**, *55*, 315.

(11) Heller, H.; Schaefer, M.; Schulten, K. *J. Phys. Chem*. **1993**, *97*, 8343.

(12) Egberts, E.; Marrink, S. J.; Berendsen, H. J. C. *Eur. Biophys. J*. **1994**, *22*, 423.

(13) Essman, U.; Perera, L.; Berkowitz, M. L. *Langmuir* **1995**, *11*, 4519.

(14) Tu, K.; Tobias, D. J.; Blaise, K.; Klein, M. L. *Biophys. J.* **1996**, *70*, 595.

(15) Huang, P.; Perez, J. J.; Loew, G. H. *J. Biomol. Struct. Dyn*. **1994**, *11*, 927.

(16) Fernandes, M. X.; Huertas, M. L.; Castanho, M. A. R. B.; García de la Torre, J. *Biochim. Biophys. Acta* **2000**, *1463*, 131.

(17) Huertas, M. L.; Cruz, V.; López Cascales, J. J.; Acuña, A. U.; García de la Torre, J. *Biophys. J.* **1996**, *71*, 1428.

(18) Mateo, C. R.; Lillo, M. P.; Gonzalez-Rodriguez, J.; Acuña, A. U. *Eur. Biophys. J*. **1991**, *20*, 53.

(19) Mateo, C. R.; Brochon, J. C.; Lillo, M. P.; Acuña, A. U. *Biophys. J*. **1993**, *65*, 2237.

(20) Sklar, L. A.; Hudson, B. S.; Simoni, R. D. *Biochemistry* **1977**, *16*, 819.

(21) Ryckaert, J. P.; Bellemans, A. *Chem. Phys. Lett.* **1975**, *30*, 123.

(22) Rey, A.; Kolinski, A.; Skolnick. J.; Levine, Y. K. *J. Chem. Phys*. **1992**, *97*, 1240.

(23) Wiener, M. C.; White, S. H. *Biophys. J*. **1992**, *61*, 434.

(24) Leermakers, F. A. M.; Scheutjens, J. M. H. M. *J. Chem. Phys.* **1988**, *89*, 6912.

(25) Yellin, N.; Levin, I. W. *Biochemistry* **1977**, *16*, 642.

(26) Ermak, D. L.; McCammon, J. A. *J. Chem. Phys*. **1978**, *69*, 1352.

(27) Iniesta, A.; García de la Torre, J. *J. Chem. Phys*. **1990**, *92*, 2015.

(28) Rotne, J.; Prager, S. *J. Chem. Phys*. **1969**, *50*, 4831.

(29) Yamakawa, H. *J. Chem. Phys*. **1970**, *53*, 436.

(30) Egberts, E.; Berendsen, H. J. C. *J. Chem. Phys.* **1988**, *89*, 3718.

(31) Lopes, S.; Fernandes; M. X.; Prieto, M.; Castanho, M. A. R. B. *J. Phys. Chem.*, in press.

(32) Kooyman, R. P. H.; Levine, Y. K.; van der Meer, B. W. *Chem. Phys*. **1981**, *60*, 317.

(33) Pottel, H.; Herreman, W.; ven der Meer, B. W.; Ameloot, M. *Chem. Phys*. **1986**, *102*, 37.

(34) Shang, Q. Y.; Dou, X.; Hudson, B. S. *Nature* (*London*) **1991**, *352*, 703.

(35) Hudson, B. S.; Cavalier, S. In *Spectroscopic membrane probes*, Vol. 1; Loew, L. M., Ed.; CRC Press Inc.: Boca Raton, FL, 1988; p 43.

(36) Provencher, S. *J. Chem. Phys*. **1976**, *64*, 2272.

(37) Provencher, S. *Biophys. J.* **1976**, *16*, 151.